HMG Advance Access published January 4, 2011

Human Molecular Genetics, 2011 **1–7**
doi:10.1093/hmg/ddq539

A key role for cyclic nucleotide gated (CNG) channels in cGMP-related retinitis pigmentosa

François Paquet-Durand[1,*], Susanne Beck[2], Stylianos Michalakis[3], Tobias Goldmann[4], Gesine Huber[2], Regine Mühlfriedel[2], Dragana Trifunović[1], M. Dominik Fischer[2], Edda Fahl[2], Gabriele Duetsch[2], Elvir Becirovic[3], Uwe Wolfrum[4], Theo van Veen[1,5], Martin Biel[3], Naoyuki Tanimoto[2] and Mathias W. Seeliger[2]

[1]Division of Experimental Ophthalmology, Institute for Ophthalmic Research, University of Tübingen, Röntgenweg 11, 72076 Tübingen, Germany, [2]Division of Ocular Neurodegeneration, Centre for Ophthalmology, Institute for Ophthalmic Research, University of Tübingen, Schleichstr. 4/3, 72076 Tübingen, Germany, [3]Munich Center for Integrated Protein Science CIPSM and Department of Pharmacy, Center for Drug Research, Ludwig-Maximilians-Universität München, Butenandtstr. 5-13, 81377 München, Germany, [4]Institute of Zoology, Cell and Matrix Biology, Johannes Gutenberg University of Mainz, Muellerweg 6, 55099 Mainz, Germany and [5]Ophthalmology Department, Clinical Sciences, University of Lund, Klinikgatan 26, BMC-B13, 22184 Lund, Sweden

Received October 25, 2010; Revised and Accepted December 6, 2010

The *rd1* natural mutant is one of the first and probably the most commonly studied mouse model for retinitis pigmentosa (RP), a severe and frequently blinding human retinal degeneration. In several decades of research, the link between the increase in photoreceptor cGMP levels and the extremely rapid cell death gave rise to a number of hypotheses. Here, we provide clear evidence that the presence of cyclic nucleotide gated (CNG) channels in the outer segment membrane is the key to rod photoreceptor loss. In *Cngb1*$^{-/-}$ × *rd1* double mutants devoid of regular CNG channels, cGMP levels are still pathologically high, but rod photoreceptor viability and outer segment morphology are greatly improved. Importantly, cone photoreceptors, the basis for high-resolution daylight and colour vision, survived and remained functional for extended periods of time. These findings strongly support the hypothesis of deleterious calcium (Ca^{2+})-influx as the cause of rapid rod cell death and highlight the importance of CNG channels in this process. Furthermore, our findings suggest that targeting rod CNG channels, rather than general Ca^{2+}-channel blockade, is a most promising symptomatic approach to treat otherwise incurable forms of cGMP-related RP.

INTRODUCTION

Retinitis pigmentosa (RP) is a group of severely disabling inherited neurodegenerative diseases. Typically, rod photoreceptor cells—permitting vision under dim light conditions—degenerate first during the course of the disease. Subsequently, the loss of rods triggers a secondary degeneration of cone photoreceptor cells, the source of high-resolution colour vision in daylight, eventually leading to complete blindness. More than 45 genes for RP have been identified so far, but the mechanisms leading to photoreceptor cell death have not been satisfactorily resolved, and at present no adequate treatment is available for practically all forms (1). The retinal degeneration 1 (*rd1* or rd) mouse model is characterized by a loss-of-function mutation in the gene encoding for the β-subunit of rod photoreceptor cGMP phosphodiesterase 6 (PDE6) (2). As a natural model for RP available before the era of genetic engineering, it has been studied extensively for several decades (3). It was found that the non-functional PDE6 leads to massive accumulation of cGMP in *rd1* rods, which via an unknown mechanism eventually causes the photoreceptors to die (4,5).

The onset of photoreceptor degeneration in *rd1* mice is exceptionally early and has a severe course, leading to an

*To whom correspondence should be addressed. Tel: +49 70712987430; Fax: +49 7071295777; Email: francois.paquet-durand@klinikum.uni-tuebingen.de

almost complete loss of the photoreceptor layer even before the retina becomes mature. Several hypotheses for the nature of this rod cell death in the presence of extremely high levels of cGMP have been developed. In photoreceptors, cGMP normally acts on cyclic nucleotide gated (CNG) ion channels, which allow for sodium and Ca^{2+}-influx associated with light-induced depolarization, and particularly an excessive Ca^{2+}-influx has been suggested to be of major importance for the pathogenesis of cGMP-related RP (Ca^{2+}-influx hypothesis). The effect on Ca^{2+} levels may be mediated either directly by cGMP action on CNG channels (6) or indirectly by activation of L-type voltage-dependent Ca^{2+} channels (VDCC) (7). However, past pharmacological and genetic approaches to block VDCCs have produced contradicting findings (7–9). The excessive levels of cGMP found in *rd1* rods would, however, also be consistent with alternative hypotheses proposing that high levels of intracellular cGMP cause cell death independent of Ca^{2+} influx, which in such a scheme would only be a secondary event (5).

Based on the assumption that Ca^{2+} influx through CNG channels is a key event in the pathophysiology of cGMP-related RP, we postulated that the ablation of these channels leads to a morphological rescue of rod photoreceptors, despite unchanged elevated cGMP levels as the mutation in PDE6 still persisted. To test for this, we cross-bred a recently described model lacking rod CNG channels due to a knockout of the *Cngb1* gene (10) with the *rd1* mouse. The resulting double-mutant animals (DBMs) were then tested functionally and morphologically, *in vivo* and *ex vivo*, and demonstrate a key role for CNG channels in rd1 photoreceptor degeneration.

RESULTS

Rod photoreceptor outer segments are preserved in DBMs

For the Ca^{2+}-influx hypothesis to be true, cGMP needs to act on functional CNG channels. At the beginning of the study, it was unclear whether this was actually possible, because *rd1* mice barely form rod outer segments, the compartment where CNG channels are localized (11). Without at least a small portion of the regular membrane area, CNG channel complexes could not be placed correctly, and thus could not facilitate any ion flux. However, both in support of the hypothesis, we found that at least rudimentary outer segments were initially present (Fig. 1A), and that the CNGB1 channel protein was produced in *rd1* animals (Fig. 1D) and expressed in rod photoreceptor outer segments (Supplementary Material, Fig. S1).

Strikingly, we found that the rod outer segments of the DBMs were much more elaborate and their morphological structure and length much closer to the normal than to the underdeveloped ones of the single mutant *rd1* mice (Fig. 1A–C). We confirmed that the CNGB1 protein was absent in DBMs in contrast to *rd1* (Fig. 1D), while cGMP levels were strongly elevated in DBM photoreceptors (Fig. 1E and F), similar to what was previously reported for *rd1* (5) (Supplementary Material, Fig. S2). Remarkably, these factors appeared to have little impact on production and ciliary transport of other outer segment proteins like rhodopsin (Fig. 1J and K).

Ablation of CNG channels rescues *rd1* retinal morphology and cone photoreceptor function *in vivo*

Next, we studied the rescue effect in the DBM line *in vivo* at postnatal day (P) 30, a stage in which the outer retina in *rd1* animals is usually completely destroyed and dysfunctional (4,11). We found that the retinal morphology was rather well preserved in the DBM animals when examined using scanning laser ophthalmoscopy (SLO) (Fig. 1I and 1G), SLO angiography and optic coherence tomography (OCT) imaging (12,13) (Supplementary Material, Fig. S3), whereas the characteristic patchy defects (Fig. 1H) indicated a severe degeneration in single-mutant *rd1* mice.

As cones have a genetically different PDE, we recorded flash electroretinograms (ERGs) under light-adapted (photopic) conditions to explore whether they were functional in contrast to rods. Figure 1L shows a comparison of the functional status of the cone system among *wt*, *rd1* and DBM mice at 5 weeks of age. Whereas no light-evoked response was detectable in *rd1* mice, substantial ERG amplitudes of about half the size of that of *wt* controls were present in DBM mice at all intensities tested. These data indicate that the structure and function of the cone system was largely preserved in *rd1* mice lacking rod CNGB1 channels.

Photoreceptor survival is increased in DBMs

We then used the TUNEL assay to look for differences in severity and timing of *rd1*-related cell death in DBM animals. In *wt* retina, developmental photoreceptor apoptosis occurred in two main phases, with peaks at around P7 and P16, in line with previous reports (14–16). While the percentage of dying cells in the *wt* ONL remained at relatively very low levels, the *rd1* mutation induced a massive photoreceptor degeneration that started already around P9 and peaked at P13 (P13 wt: $0.046 \pm 0.008\%$ SEM; P13 *rd1*: $5.22 \pm 0.54\%$ SEM, $n = 5$, $P < 0.001$). Single $Cngb1^{-/-}$ animals also suffered from retinal photoreceptor degeneration, albeit at a much slower rate, with a peak of cell death at around P24. In terms of photoreceptor cell death, the $Cngb1^{-/-} \times rd1$ DBM displayed an intermediate phenotype with a delayed onset of degeneration (dying ONL cells in P13 DBM: $2.15 \pm 0.20\%$ SEM, $n = 5$, $P = 0.040$), a progression that was slower than *rd1* but faster than $Cngb1^{-/-}$, and a peak of cell death at P18 (Fig. 2A–E).

This was also reflected in the number of rows of photoreceptor nuclei in the outer retina over time, a measure of the fraction of surviving cells (Fig. 2G). Specifically, about half of the DBM photoreceptors survived at P60, whereas practically all had vanished in the *rd1* single mutant (DBM: 4.7 rows $\pm$ 0.7 SEM; *rd1*: 0.9 ± 0.3, $P = 0.017$).

To further probe the nature of the degeneration, we went on to study calpain activity. Calpains are Ca^{2+}-activated cysteine-type proteases that have been implicated in many forms of neurodegeneration (17), including in the retina (18). The activity of calpains essentially followed the pattern of cell death in the different genotypes (Fig. 2F), with one remarkable

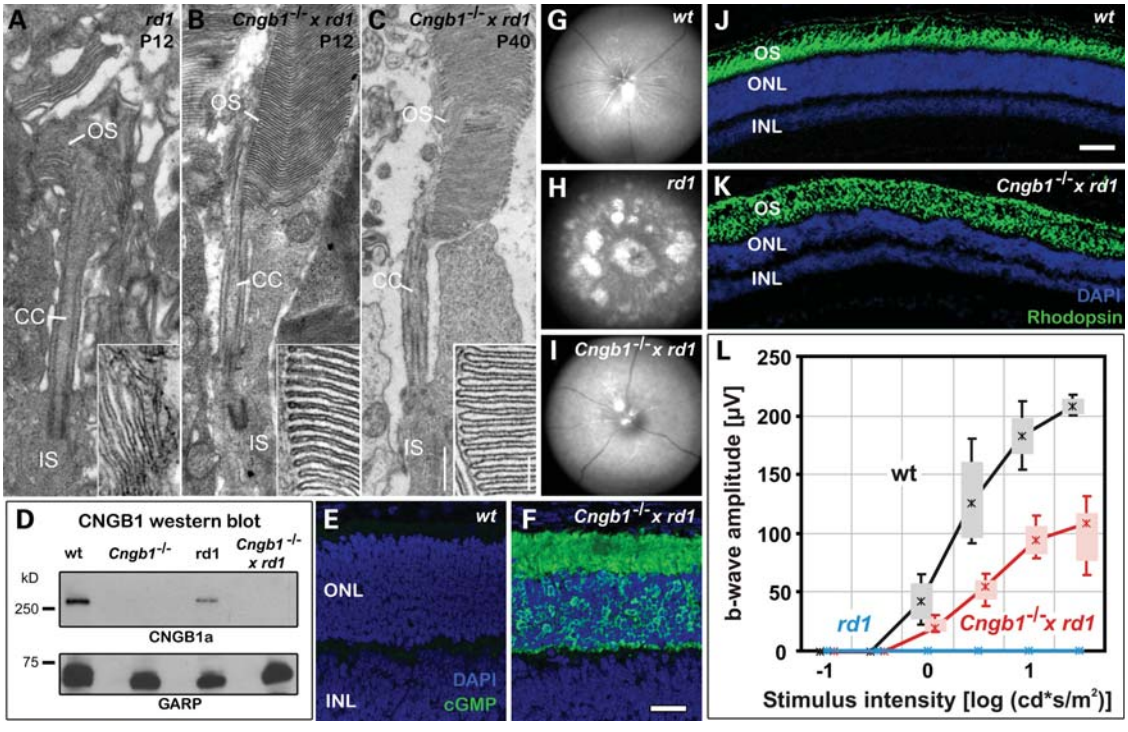

Figure 1. Retinal morphology and function is preserved in *rd1* animals lacking CNGB1. (**A–C**) Electron microscopy of rod outer segment structure shows (A) incomplete development of *rd1* rod outer segments at P12. (B) Rod outer segments in *Cngb1*$^{-/-}$ × *rd1* double-mutant (DBM) retina appear mildly disorganized at P12 but otherwise normal even though CNGB1 channel protein is not expressed. (C) At P40 outer segments in DBM retina appear still almost normal, highlighting the persistence of the structural improvement. CC, connecting cilium; OS, outer segment; IS, inner segment. Scale bar = 500 nm (inset 100 nm). (**D**) Western blot of CNGB1 protein in P12 *wt*, *rd1*, *Cngb1*$^{-/-}$ and DBM mice. CNG channels are present in *wt* and, to a lower extent, due to the smaller membrane surface, in *rd1* mice. (**E** and **F**) DAPI/cGMP double immunostaining in photoreceptors at P18 shows (E) no excessive cGMP accumulation in *wt* photoreceptors, whereas (F) cGMP levels are highly elevated in DBM retina. Scale bar = 50 µm. (**G–I**) Retinal *in vivo* morphology at P30 assessed by scanning-laser ophthalmoscopy (SLO) at 514 nm. (G) Normal fundus of a *wt* animal. (H) Typical widespread, patchy changes in *rd1* mutants indicating severe retinal degeneration. (I) Minor discolorations are present in the fundus of DBM animals. (**J** and **K**) Rhodopsin content in photoreceptors at P30. (J) *wt* control; scale bar = 100 µm. (K) DBM mouse. (I) Extended preservation of cone function in DBM mice at P30. Photopic single flash ERG b-wave amplitudes in *wt* (black), *rd1* (blue) and DBM (red) mice as a function of the logarithm of flash intensity. Boxes indicate the 25–75% quantile range, whiskers the 5% and 95% quantiles and solid lines connect the medians of the data.

difference: while in the *rd1* retina calpain activity positive cells outnumbered TUNEL positive cells by approximately 2:1, this situation was reversed in *Cngb1*$^{-/-}$ single- and DBMs where the ratio of calpain activity to cell death was at roughly 1:2 (Fig. 2H).

DISCUSSION

Retinal degenerations, particularly of the RP group, are severe, blinding neurodegenerative diseases of vision and currently incurable. The disclosure of the underlying pathophysiology and the development of treatment strategies strongly rely on animal models carrying homologous genetic defects. Even though the *rd1* mouse is one of the earliest known animal models for RP, the mechanisms underlying its extremely fast photoreceptor degeneration have puzzled scientists for decades. Our findings attribute a pivotal role in the degenerative process to CNG channels. Importantly, genetic ablation of rod photoreceptor CNG channels preserved rod viability while at the same time rescuing cone photoreceptor function.

One of the most prominent and best-studied features of *rd1* mice is the massive photoreceptor cell death (1). The photoreceptor rescue observed in the DBM retina was relatively large to what has previously been achieved, for example, by genetic deletion of the β2 subunit of VDCC (19,20). In VDCCb2$^{-/-}$ × *rd1* DBM, the ONL at PN18 was found to be only 0.3-fold thicker than in *rd1* single mutants (20), compared with 2.9-fold increase in thickness in the CNGb1$^{-/-}$ × *rd1* DBM at the same age.

rd1 photoreceptor cell death is associated with and causally connected to excessive activation of calpain-type proteases (21,22). The finding that calpain activity was strongly reduced in the DBM is compatible with the idea that the absence of CNG channels decreases intracellular Ca^{2+} levels and hence reduces calpain activity (18), and is also in agreement with results on improved photoreceptor survival afforded by different types of Ca^{2+}-channel blockers (23).

We conclude from these results that elevated cGMP levels by itself do not cause much of the pathology observed in *rd1* mice. Rather, the combination with CNG channels is needed to produce a severe disease phenotype. CNG channels may also be involved in disease mechanisms in other models for RP (24) and achromatopsia (25,26). Our results suggest that the rudimentary outer segment in *rd1* animals provides

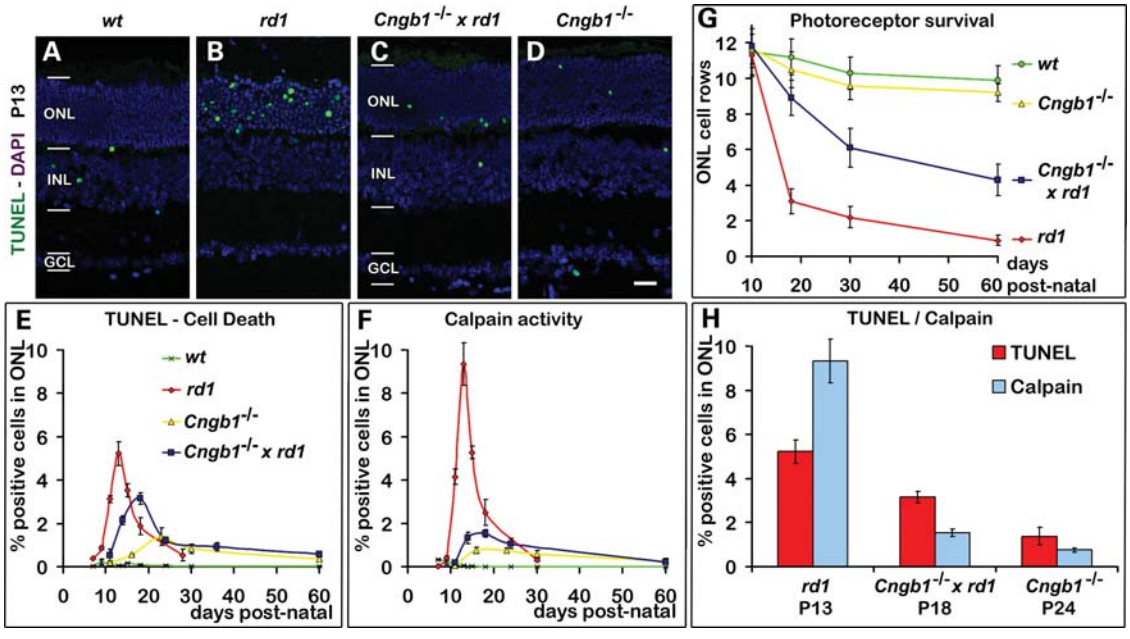

Figure 2. Cell death and calpain activity are strongly decreased in DBMs. (**A–E**) Comparison of TUNEL assays in *wt*, *rd1*, *Cngb1*$^{-/-}$ and DBM animals at P13. (A) Very few cells were TUNEL positive in *wt* retina (B), while in the *rd1* situation at about the peak of cell death a large number of ONL cells were TUNEL positive. (C) The numbers of dying cells were strongly reduced in DBM mice (D), and even lower in *Cngb1*$^{-/-}$ mice; scale bar = 25 μm. (E) Time course of TUNEL positivity. In comparison to *rd1*, the peak of cell death in DBM animals was delayed to PN18 and the peak height strongly reduced. (**F–H**) Activity of Ca^{2+}-dependent, calpain-type proteases in different genotypes. (F) Time course of calpain activity showing a dramatic reduction of calpain activity in DBM animals when compared with rd1. (H) Bar graph detail of P13–P24. Interestingly, at the respective peaks of degeneration, the ratio of calpain activity to cell death was reversed from approximately 2:1 in the *rd1* situation to 1:2 in the double mutant and *Cngb1*$^{-/-}$.

sufficient membrane area for the deleterious effect mediated by the CNG channels. Intriguingly, the previously observed deleterious effect of over-activation of cGMP-dependent PKG on photoreceptors (5) may also depend on CNG channel activity, since PKG activity may directly or indirectly modulate CNG channel conductivity (27).

Our data may further help to understand the mechanism that slowed photoreceptor degeneration in *rd1* × *rd2* DBMs (28) compared with *rd1* mutants alone. The *rd2* (rds) mutant suffers from a lack of expression of the scaffolding protein peripherin leading to an absence of outer segments (29). In the light of our results, the lack of outer segment formation in the *rd2* line lead to a lack of CNG channels in the *rd1* × *rd2* double mutants, which in turn considerably retards retinal degeneration despite massive accumulation of rod cGMP (30).

Taken together, the removal of CNG channels in *rd1* and CNGB1 double-mutant mice led to the most complete rescue of the retinal phenotype of *rd1* mice so far observed by any group. The morphological preservation of rods allowed for an extended survival of cones, yielding substantial vision-related signals at 5 weeks after birth and beyond. This functional rescue of cone photoreceptors may be particularly interesting for the human situation where high resolution, daylight vision depends on cone function. Our study provides strong evidence for the link between Ca^{2+} influx and rod cell death, rendering modulation of rod CNG channel activity a most promising target for the treatment in retinal degenerations with elevated cellular levels of cGMP.

MATERIALS AND METHODS

Animals

Animals were housed under standard white cyclic lighting, had free access to food and water and were used irrespective of gender. All procedures were performed in accordance with the local Tübingen University animal care and protection committee (§4 registrations from 23 January 2008 and 12 March 2010) and the ARVO statement for the use of animals in ophthalmic and visual research. All efforts were made to minimize the number of animals used and their suffering.

Generation of DBMs, confirmation of geno- and proteotype

Cngb1$^{-/-}$ *rd1*/*rd1* double mutants were generated by cross-breeding *Cngb1*$^{-/-}$ mice on a 129SvJ and C57BL/6N background (10) with C3H mice (11) which carry a retinal degeneration mutation caused by a proviral insertion into the *Pdeb* gene, encoding the β-subunit of cGMP PDE6. The F4 progenies of *Cngb1*$^{-/-}$ × *rd1* mice were used for this study. Transgene determination of the *Cngb1* gene was performed by multiplex PCR as described previously (10). Based on a database search, three oligonucleotides were devised to distinguish mutant *rd1* and *wt* alleles at the Pde6b locus: Pde6b-f-*wt*: 5′-CCACCTTCAGGGAATCTTCA-3′ (MGI:97525), Pde6b-r-*wt*: 5′-CTCAGTTTGCCTCTCGCT-3′ (MGI:97525, www.informatics.jax.org) and *rd1*-r: 5′-CCTTGCAAAATGGCGTTACT (NCBI, Accession L02109). Multiplex PCR analysis with genomic DNA using primers Pde6b-f-*wt*/Pde6b-r-*wt*/*rd1*-r yielded a 429 bp

fragment for *wt* and a 265 bp for the proviral insertion. Correct genotypes were confirmed using PCR (Supplementary Material, Fig. S1). Western blot and immunofluorescence were used to confirm the proteotype of *Cngb1*$^{-/-}$ × *rd1* animals, showing that these animals express neither CNGB1 nor PDE6b protein (Supplementary Material, Fig. S1).

In vivo testing: SLO, OCT, ERG

SLOs were obtained as reported previously (12,13). Briefly, mice were anaesthetized by subcutaneous injection of ketamine (66.7 mg/kg) and xylazine (11.7 mg/kg). After anaesthesia, pupils were dilated with tropicamide eye drops (Mydriaticum Stulln, Pharma Stulln, Stulln, Germany). SLO imaging was performed with a Heidelberg Retina Angiograph (HRA I). Fluorescein angiography was performed using an s.c. injection of 75 mg/kg body weight fluorescein-Na. Spectral domain optical coherence tomography (OCT) imaging was done in the same session as ERG, i.e. animals remained anaesthetized. Mouse eyes were subjected to OCT using a Spectralis^{TM} HRA + OCT device from Heidelberg Engineering. Optical depth resolution is ca. 7 μm with digital resolution reaching 3.5 μm (12). Imaging data were analysed using the proprietary software package Eye Explorer version 3.2.1.0 from Heidelberg Engineering. Resulting data were exported as 24 bit colour image files and processed in Adobe Photoshop CS3 (Adobe Systems, San Jose, CA, USA) (12,31).

ERGs were recorded according to the previously described procedures (32,33). Single flash intensity series data were obtained under photopic (light-adapted 10 min at 30 cd/m^2) conditions. Flash stimuli ranged from −2.0 to 1.5 log cd*s/m^2 divided into eight steps. All animals were analysed at 5 weeks of age.

Transmission electron microscopy

Tissue preparation for transmission electron microscopy was performed as previously described (34). Briefly, eyes were fixed in 2.5% glutaraldehyde in 0.1 M Cacodylate buffer (pH 7.3) for 2 h at RT. Specimens were washed and fixed in buffered 2% OsO_4, dehydrated and embedded in araldite. Semi-thin (0.5 μm) and ultra-thin (60 nm) sections were cut on a Leica Ultracut S microtome. Ultrastructural analyses were performed using a Tecnai 12 BioTwin transmission electron microscope (FEI, Eindhoven, The Netherlands) and imaged with a SIS MegaView III SCCD camera.

Immunostaining and western blot

Paraformaldehyde fixed retinal cryosections were dried for 30 min at 37°C, rehydrated in PBS and pre-incubated for 1 h at RT in blocking solution, containing 10% normal serum and 0.1% Triton in PBS (PBST). Immunofluorescence was performed overnight at 4°C, using primary antibodies diluted in blocking solution (see Table 1). The tissue was rinsed with PBST, and incubated for 1 h with corresponding secondary antibody, conjugated to either Alexafluor 488 or 568 (1:200-1:750, Invitrogen, Carlsbad, CA, USA), diluted in PBST. Sections were rinsed in PBS, and mounted in Vectashield with DAPI (Vector Laboratories Inc., Burlingame, CA, USA). For negative controls, in addition to the use of *rd1* and CNGb1 mutant retina, the primary antibodies were omitted. Western blotting for CNGb1 protein was performed as previously described (10).

Table 1. Antibodies used in this study

Antibody	Source/manufacturer	Dilution	Reference
Sheep anti-cGMP	Harry Steinbusch, University of Maastricht, The Netherlands	1:500	(36)
Rabbit anti-CNGB1	Martin Biel, University of Munich, Germany	1:30.000	(10)
Mouse anti-rhodopsin, Ab-1 (Clone RET-P1)	Lab Vision, Fremont, CA, USA	1:50	(10)
Rabbit anti-PDE6 β	Thermo Fisher Scientific, Bonn, Germany	1:100	(37)

TUNEL assay

The terminal deoxynucleotidyl transferase dUTP nick end labelling (TUNEL) assay was performed on retinal cryosections, using an *in situ* cell death detection kit conjugated with fluorescein isothiocyanate (Roche Diagnostics, Mannheim, Germany). As control, terminal deoxynucleotidyl transferase enzyme was either omitted from the labelling solution (negative control), or sections were pre-treated for 30 min with DNAse I (Roche, 3 U/ml) in 50 mM Tris–HCl, pH 7.5, 1 mg/ml BSA to induce DNA strand breaks (positive control). Negative control gave no staining at all, while positive control stained all nuclei in all layers of the retina (35).

Calpain activity assay

Tissue sections from unfixed retinas were incubated for 15 min in calpain reaction buffer (CRB: 25 mM HEPES, 65 mM KCl, 2 mM $MgCl_2$, 1.5 mM $CaCl_2$, 2 mM DTT, pH 7.2). The fluorescent calpain substrate CMAC, t-BOC-Leu-Met (A6520, Invitrogen) was then added to CRB at a final concentration of 2 μM and incubated in the dark for 2 h at 37°C. The sections were washed twice for 10 min in CRB and then mounted with Vectashield. The activity assay generally labelled the cell membranes, with calpain-activity-positive cells additionally showing a bright labelling of the nucleus and perinuclear cytoplasm.

Microscopy, cell counting and statistics

Morphological observations and routine light microscopy were performed on a Zeiss Imager Z1 Apotome Microscope, equipped with a Zeiss Axiocam digital camera. Images were captured using Zeiss Axiovision 4.7 software; image overlays and contrast enhancement were done using Adobe Photoshop CS3. Images shown in figures are representative for at least three different animals for each genotype/treatment. Percentages of TUNEL and calpain activity positive cells were assessed and calculated in a blinded fashion as reported previously (5,35). The mean value for photoreceptor rows in

the ONL after *in vitro* culture was determined using DAPI nuclear counterstaining. Values are given as mean ± standard error of the mean (SEM). Statistical significance was tested using Student's paired, two-tailed *t*-test and GraphPad Prism software (La Jolla, CA, USA).

SUPPLEMENTARY MATERIAL

Supplementary Material is available at *HMG* online.

ACKNOWLEDGEMENTS

We thank K. Dengler, S. Bernhard-Kurz, F. Sehn, J. Schmidt and G. Utz for excellent technical assistance and B. Wissinger and T. Euler for helpful comments and discussions.

Conflict of Interest statement. None declared.

FUNDING

This work was supported by grants from the Deutsche Forschungsgemeinschaft (DFG Se837/5-2, Se837/6-1, Se837/7-1 and Pa1751/1-1); the German Ministry of Education and Research (BMBF 0314106); the European Union (EU; HEALTH-F2-2008-200234 and NEUROTRAIN: MEST-CT-2005-020235); Centre for Integrative Neuroscience (CIN; pool project 2009-20); the Charlotte and Tistou Kerstan Foundation; and the FAUN Foundation.

REFERENCES

1. Sancho-Pelluz, J., Arango-Gonzalez, B., Kustermann, S., Romero, F.J., van Veen, T., Zrenner, E., Ekström, P. and Paquet-Durand, F. (2008) Photoreceptor cell death mechanisms in inherited retinal degeneration. *Mol. Neurobiol.*, **38**, 253–269.
2. Bowes, C., Li, T., Danciger, M., Baxter, L.C., Applebury, M.L. and Farber, D.B. (1990) Retinal degeneration in the rd mouse is caused by a defect in the beta subunit of rod cGMP-phosphodiesterase. *Nature*, **347**, 677–680.
3. Keeler, C.E. (1924) The inheritance of a retinal abnormality in white mice. *Proc. Natl Acad. Sci. USA*, **10**, 329–333.
4. Farber, D.B. and Lolley, R.N. (1974) Cyclic guanosine monophosphate: elevation in degenerating photoreceptor cells of the C3H mouse retina. *Science*, **186**, 449–451.
5. Paquet-Durand, F., Hauck, S.M., van Veen, T., Ueffing, M. and Ekström, P. (2009) PKG activity causes photoreceptor cell death in two retinitis pigmentosa models. *J. Neurochem.*, **108**, 796–810.
6. Fox, D.A., Poblenz, A.T. and He, L. (1999) Calcium overload triggers rod photoreceptor apoptotic cell death in chemical-induced and inherited retinal degenerations. *Ann. N. Y. Acad. Sci.*, **893**, 282–285.
7. Frasson, M., Sahel, J.A., Fabre, M., Simonutti, M., Dreyfus, H. and Picaud, S. (1999) Retinitis pigmentosa: rod photoreceptor rescue by a calcium-channel blocker in the rd mouse. *Nat. Med.*, **5**, 1183–1187.
8. Pawlyk, B.S., Li, T., Scimeca, M.S., Sandberg, M.A. and Berson, E.L. (2002) Absence of photoreceptor rescue with D-cis-diltiazem in the rd mouse. *Invest. Ophthalmol. Vis. Sci.*, **43**, 1912–1915.
9. Pearce-Kelling, S.E., Aleman, T.S., Nickle, A., Laties, A.M., Aguirre, G.D., Jacobson, S.G. and Acland, G.M. (2001) Calcium channel blocker D-cis-diltiazem does not slow retinal degeneration in the PDE6B mutant rcd1 canine model of retinitis pigmentosa. *Mol. Vis.*, **7**, 42–47.
10. Hüttl, S., Michalakis, S., Seeliger, M., Luo, D.G., Acar, N., Geiger, H., Hudl, K., Mader, R., Haverkamp, S., Moser, M. *et al.* (2005) Impaired channel targeting and retinal degeneration in mice lacking the cyclic nucleotide-gated channel subunit CNGB1. *J. Neurosci.*, **25**, 130–138.
11. Sanyal, S. and Bal, A.K. (1973) Comparative light and electron microscopic study of retinal histogenesis in normal and rd mutant mice. *Z. Anat. Entwicklungsgesch.*, **142**, 219–238.
12. Huber, G., Beck, S.C., Grimm, C., Sahaboglu-Tekgoz, A., Paquet-Durand, F., Wenzel, A., Humphries, P., Redmond, T.M., Seeliger, M.W. and Fischer, M.D. (2009) Spectral domain optical coherence tomography in mouse models of retinal degeneration. *Invest. Ophthalmol. Vis. Sci.*, **50**, 5888–5895.
13. Seeliger, M.W., Beck, S.C., Pereyra-Munoz, N., Dangel, S., Tsai, J.Y., Luhmann, U.F., van de Pavert, S.A., Wijnholds, J., Samardzija, M., Wenzel, A. *et al.* (2005) In vivo confocal imaging of the retina in animal models using scanning laser ophthalmoscopy. *Vision Res.*, **45**, 3512–3519.
14. Schoppner, A. and Kindl, H. (1984) Purification and properties of a stilbene synthase from induced cell suspension cultures of peanut. *J. Biol. Chem.*, **259**, 6806–6811.
15. Young, R.W. (1984) Cell death during differentiation of the retina in the mouse. *J. Comp. Neurol.*, **229**, 362–373.
16. Mervin, K. and Stone, J. (2002) Developmental death of photoreceptors in the C57BL/6J mouse: association with retinal function and self-protection. *Exp. Eye Res.*, **75**, 703–713.
17. Hanna, R.A., Campbell, R.L. and Davies, P.L. (2008) Calcium-bound structure of calpain and its mechanism of inhibition by calpastatin. *Nature*, **456**, 409–412.
18. Paquet-Durand, F., Johnson, L. and Ekström, P. (2007) Calpain activity in retinal degeneration. *J. Neurosci. Res.*, **85**, 693–702.
19. Ball, S.L., Powers, P.A., Shin, H.S., Morgans, C.W., Peachey, N.S. and Gregg, R.G. (2002) Role of the beta(2) subunit of voltage-dependent calcium channels in the retinal outer plexiform layer. *Invest. Ophthalmol. Vis. Sci.*, **43**, 1595–1603.
20. Read, D.S., McCall, M.A. and Gregg, R.G. (2002) Absence of voltage-dependent calcium channels delays photoreceptor degeneration in rd mice. *Exp. Eye Res.*, **75**, 415–420.
21. Paquet-Durand, F., Azadi, S., Hauck, S.M., Ueffing, M., van Veen, T. and Ekström, P. (2006) Calpain is activated in degenerating photoreceptors in the rd1 mouse. *J. Neurochem.*, **96**, 802–814.
22. Paquet-Durand, F., Sanges, D., McCall, J., Silva, J., van Veen, T., Marigo, V. and Ekström, P. (2010) Photoreceptor rescue and toxicity induced by different calpain inhibitors. *J. Neurochem.*, **115**, 930–940.
23. Takano, Y., Ohguro, H., Dezawa, M., Ishikawa, H., Yamazaki, H., Ohguro, I., Mamiya, K., Metoki, T., Ishikawa, F. and Nakazawa, M. (2004) Study of drug effects of calcium channel blockers on retinal degeneration of rd mouse. *Biochem. Biophys. Res. Commun.*, **313**, 1015–1022.
24. Tosi, J., Davis, R.J., Wang, N.K., Naumann, M., Lin, C.S. and Tsang, S.H. (2010) shRNA knockdown of guanylate cyclase 2e or cyclic nucleotide gated channel alpha 1 increases photoreceptor survival in a cGMP phosphodiesterase mouse model of retinitis pigmentosa. *J. Cell Mol. Med.*, [Epub ahead of print]. doi: 10.1111/j.1582-4934.2010.01201.x.
25. Michalakis, S., Muhlfriedel, R., Tanimoto, N., Krishnamoorthy, V., Koch, S., Fischer, M.D., Becirovic, E., Bai, L., Huber, G., Beck, S.C. *et al.* (2010) Restoration of cone vision in the CNGA3$(^{-/-})$ mouse model of congenital complete lack of cone photoreceptor function. *Mol. Ther.*, **18**, 2057–2063.
26. Trifunovic, D., Dengler, K., Michalakis, S., Zrenner, E., Wissinger, B. and Paquet-Durand, F. (2010) cGMP-dependent cone photoreceptor degeneration in the cpfl1 mouse retina. *J. Comp. Neurol.*, **518**, 3604–3617.
27. Castro, L.R., Schittl, J. and Fischmeister, R. (2010) Feedback control through cGMP-dependent protein kinase contributes to differential regulation and compartmentation of cGMP in rat cardiac myocytes. *Circ. Res.*, **107**, 1232–1240.
28. Fletcher, R.T., Sanyal, S., Krishna, G., Aguirre, G. and Chader, G.J. (1986) Genetic expression of cyclic GMP phosphodiesterase activity defines abnormal photoreceptor differentiation in neurological mutants of inherited retinal degeneration. *J. Neurochem.*, **46**, 1240–1245.
29. Goldberg, A.F. (2006) Role of peripherin/rds in vertebrate photoreceptor architecture and inherited retinal degenerations. *Int. Rev. Cytol.*, **253**, 131–175.
30. Sanyal, S. and Hawkins, R.K. (1981) Genetic interaction in the retinal degeneration of mice. *Exp. Eye Res.*, **33**, 213–222.
31. Fischer, M.D., Huber, G., Beck, S.C., Tanimoto, N., Muehlfriedel, R., Fahl, E., Grimm, C., Wenzel, A., Reme, C.E., van de Pavert, S.A. *et al.*

(2009) Noninvasive, *in vivo* assessment of mouse retinal structure using optical coherence tomography. *PLoS ONE*, **4**, e7507.
32. Tanimoto, N., Muehlfriedel, R.L., Fischer, M.D., Fahl, E., Humphries, P., Biel, M. and Seeliger, M.W. (2009) Vision tests in the mouse: functional phenotyping with electroretinography. *Front Biosci.*, **14**, 2730–2737.
33. Seeliger, M.W., Zrenner, E., Apfelstedt-Sylla, E. and Jaissle, G.B. (2001) Identification of Usher syndrome subtypes by ERG implicit time. *Invest. Ophthalmol. Vis. Sci.*, **42**, 3066–3071.
34. Wolfrum, U. (1992) Cytoskeletal elements in arthropod sensilla and mammalian photoreceptors. *Biol. Cell*, **76**, 373–381.
35. Paquet-Durand, F., Silva, J., Talukdar, T., Johnson, L.E., Azadi, S., van Veen, T., Ueffing, M., Hauck, S.M. and Ekström, P.A. (2007) Excessive activation of poly(ADP-ribose) polymerase contributes to inherited photoreceptor degeneration in the retinal degeneration mouse 1. *J. Neurosci.*, **27**, 10311–10319.
36. De Vente, J., Steinbusch, H.W. and Schipper, J. (1987) A new approach to immunocytochemistry of 3',5'-cyclic guanosine monophosphate: preparation, specificity, and initial application of a new antiserum against formaldehyde-fixed 3′,5′-cyclic guanosine monophosphate. *Neuroscience*, **22**, 361–373.
37. Guo, L.W., Grant, J.E., Hajipour, A.R., Muradov, H., Arbabian, M., Artemyev, N.O. and Ruoho, A.E. (2005) Asymmetric interaction between rod cyclic GMP phosphodiesterase gamma subunits and alphabeta subunits. *J. Biol. Chem.*, **280**, 12585–12592.